IRAQI JOURNAL OF APPLIED PHYSICS
Vol. (14), No. (4), October-December 2018, pp. 25-28

Formation of Mid-Infrared Slot Antenna Arrays on Thin Al_2O_3/Si Structures Fabricated by Atomic Layer Deposition

Amjd A. Salman
Malik S. Ashoor

Department of Electric and Electronic Engineering, College of Engineering, Alqadisiya University, Diwaniya, IRAQ

The vertical distribution of the electric field enhancement produced by optical antennas could be experimentally confirmed. The combination of the antenna and a quantum cascade laser would yield attractive mid-infrared microscopic analysis to detect a solid state surface. In this work, slot antenna arrays were formed on a thin Al_2O_3 layer grown by atomic layer deposition on a silicon substrate. Reflectivity spectra measured in the mid-infrared range showed characteristic aspects, presumably caused by the surface phonon polariton of a SiO_2 layer naturally formed on the Si substrate. When the Al_2O_3 layer thickness was 6 nm, such spectral features disappeared. In this way, we could estimate experimentally the electric field distribution normal to the surface of the substrate.

Keywords: Copper oxide; Catalyst; XAFS; Electron yield detection
Received: 15 August 2018; **Revised:** 26 August 2018; **Accepted:** 2 September 2018

1. Introduction

Wide band antenna design has become a challenging topic [1] with the gradual progress of wireless communication systems and in the increase in their applications. Wide-slot antennas have now proven as the panacea for larger bandwidth because they have two orthogonal resonance modes, which are merged to create a wide impedance bandwidth [2]. Thus, printed slot antennas have now gain a great popularity among the researchers. Antennas with various shapes such as circle [3], ellipse [4], and triangle [5] were reported for wide bandwidth requiring each slot shape a feed stub of appropriate shape. An optimum impedance bandwidth can be gained by the coupling between the feeding structure and the slot [6-9]. In reference [6], a printed wide-slot antenna fed by a microstrip line with a fork-like tuning stub provided broad bandwidth through the proper parameters of the fork-like tuning stub. An L-shaped slot [7] with a W-shaped feed stub can improve bandwidth. In references [10] and [11] a novel technique for bandwidth enhancement has been provided for a microstrip-fed wide-slot antenna based on fractal shapes. Significant bandwidths enhancement of the proposed wide-slot antenna was achieved by etching a wide slot as fractal shapes though the design specifications of the wide-slot antenna is more complicated. The applicability of square slot antenna is greater owing to its relatively wider bandwidth than other types of antennas, but with respect to a broadband antenna it finds limitation due to the characteristics of a single resonant mode. In reference [12], by rotating the square slot, the other resonant mode operating near one of a conventional wide-slot antenna can be obtained. However, it was not enough for the operating bandwidth to cover more wireless communication services. Fractal antenna geometry configurations are discussed in some papers as to provide more compactness [13-16] .Thus fractal shaped defects are successfully incorporated in the patch to provide more compactness so to be tuned to lower operative frequency.

Optical antennas can enhance local field intensity. The field intensity becomes large near the antenna, which, however, falls drastically at positions distant from it, indicating an occurrence of intense localization of electric fields near the antenna, and hence, the generation of an optical hotspot. The distribution of the electric field around an optical antenna can be calculated by finite-difference time-domain (FDTD), and it is possible to know the field enhancement effect of the antenna by observing the reflection spectra with the use of a Fourier transform infrared (FT-IR) spectrometer [17]. If one could use, for example, scattering near-field microscopy (s-SNOM) [18], local information on the field enhancement on a plane would be available. However, such information obtained in a certain position includes data in both horizontal and vertical directions. Very little experimental work showing the field enhancement distribution of the antenna in a vertical direction is currently available in published literature. Towards that end, a thin dielectric layer was deposited on a Si substrate with the use of atomic layer deposition (ALD), and dumbbell-shaped slot antennas were fabricated on it. It was possible to grow the layer with the thickness being controlled to an accuracy of ~1 nm. By observing the spectra reflected off antenna arrays with different layer thicknesses, an understanding of the vertical field distribution could be gained (i.e.

the field localization and the magnitude of the field enhancement).

2. Experimental Part

The shape of a conventional slot antenna is rectangular. In this study, it was modified like a dumbbell so as to increase field-intensity near the feed gap at the center, and to form a single hot spot [19-21]. Another merit of these antennas is that the fabrication is easier than that of dipole antennas, because dipole antennas leave small metal stripes on a substrate. The antenna arrays were fabricated as follows: a thin Al_2O_3 was grown using the ALD on a Si substrate. A set of cleaning processes including HF treatment is ordinarily performed to remove an oxide film naturally formed on a Si substrate prior to deposition of dielectric layers. In this study, that process was omitted. Next, Au (40nm)/Ti (10nm) were deposited on the substrate. Antenna patterns were made by electron-beam lithography and a lift-off technique followed it, cutting out dumbbell-shaped openings from the metal sheet. One antenna array consisted of 15x5 elements with each having the same size and dimensions. Besides the antenna arrays, the metal sheet had 30x30 μm square openings to examine the antenna effect.

3. Results and Discussions

The reflection spectrum of one antenna array was measured using a microscopic FT-IR, which is in the IR microscope beamline (BL-15) in the SR center. A globar lamp in the FT-IR was used as IR light source and an aperture size was 24x24 μm. The reflection spectrum was normalized by the reflectivity from the Au film on the substrate. Figure (1a) shows the plain view and cross-section view of an antenna element, and Fig. (1b) shows the normalized spectra of three arrays. The lengths of the elements in three arrays were 1, 1.5 and 2 μm. The polarization of incident light was perpendicular to the length direction, which was the resonant direction of antennas. The normalized reflectivity of the square opening (i.e. region without antenna elements) is also shown in Fig. (1b). While the reflection spectrum of the square opening decreased monotonously over the range from 750 to 1750 cm^{-1}, the arrays showed distinctly different spectra. Although as L was increased, the resonance wavenumbers of the arrays became small, one can see that the reflectivity grew in the range between ~1075 cm^{-1} and ~1250 cm^{-1}.

Figure (2a) shows the results for antenna arrays on an Al_2O_3/Si substrate. The thicknesses of Al_2O_3 were 0, 2, 4, and 6 nm. The dip appearing around 1250 cm^{-1} weakened as the Al_2O_3 was thick, and for 6 nm, it disappeared. The measured reflectivity of the square opening region, shown in Fig. (1b), reflects the optical properties of silicon bulk. Field enhancement occurs in the vicinity of antennas, and even taking into consideration the antenna resonance properties, the spectra of the arrays were completely dissimilar. Therefore, it is reasonably concluded that the characteristic spectral change appearing in the arrays were caused by a thin SiO_2 layer naturally formed on the Si substrate.

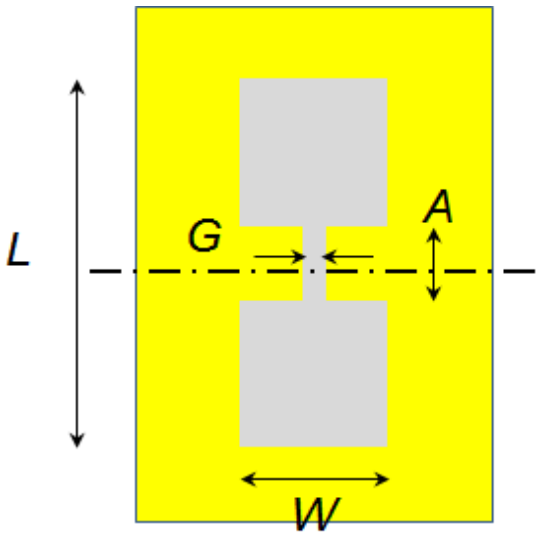

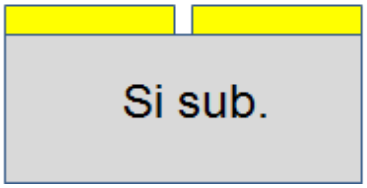

(a)

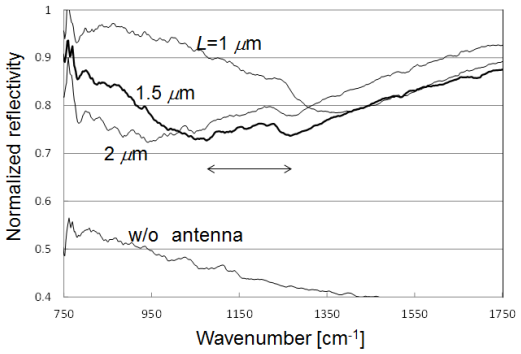

(b)

Fig. (1) Antenna arrays on a silicon substrate. (a) Plain view (top) and cross-section view (bottom) of one element. *W*=0.6μm, *A*=0.4μm, and *G*=0.1μm. (b) Reflection spectra by microscopic FTIR. Each array consisted of 15x5 dumbbell-shaped elements. A horizontal arrow indicates the rage from 1075 cm^{-1} to 1250 cm^{-1}

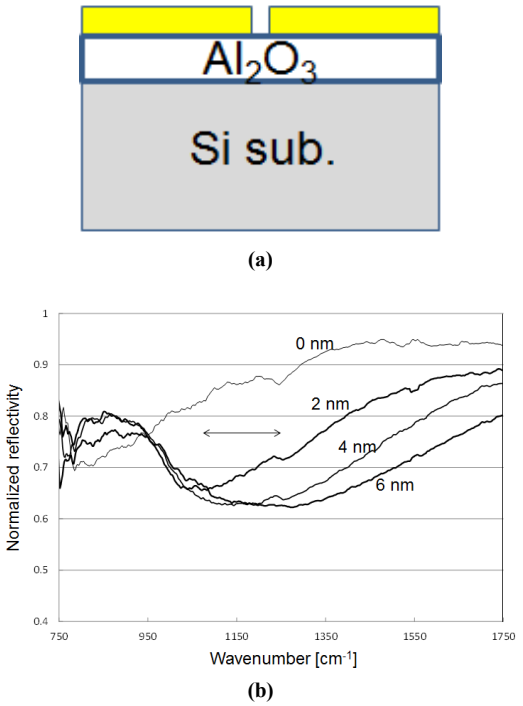

Fig. (2) Antenna arrays on an Al_2O_3/Si substrate. (a) Cross-section view. *L*=2.5µm, *W*=0.6µm, *A*=0.2µm, and *G*=0.1µm. (b) Reflection spectra for Al_2O_3 having thicknesses of 0, 2, 4, and 6 nm

Similar dip was reported to appear around 1250cm^{-1} in FTIR transmission spectra in ref. [21], where it was attributed to the surface phonon polariton (SPHP). Aside from the substrates mentioned above, antenna arrays fabricated on a CVD-SiO_2 (50nm)/Si substrate were also made, which showed a broad dip around 1065 cm^{-1}. This wavenumber almost coincided with the transverse optical frequency (ωT) of SiO_2. From these results, the dips that appeared around 1075 cm^{-1} and 1250 cm^{-1} are presumed to arise from the SPHP of a natural SiO_2 layer, corresponding to two SPHP modes which appear when the layer thickness is thin and has two interfaces [22]. In the case of phonon polariton in bulk, the frequency range between ωT<ω<ωL (longitudinal optical frequency) becomes a stop band. The reflectivity increases in that range, because photons are prohibited from being present. Two SPHP frequencies exist within the stop band. For the SPHP modes to appear, it is necessary that the straight line expressing the dispersion in the air must intersect the dispersion curves of the two-interface SPHP. A parallel wave number of the SPHP modes approaches ω/*c* as ω comes close to ωT. Although incident light entered obliquely on the arrays in the FT-IR, allowing the existence of a parallel electric component (i.e. polarization direction: perpendicular to the substrate surface), this still seems difficult to achieve, because the dispersion in the air was ω=*cq*/sinθ, not satisfying the condition of ω<*cq*(*c*: light speed, *q*: wave number, and θ: angle measured from normal line). However, the authors believe that it is not the case when antennas are formed. It would be necessary to take in the effect of slow light due to the antenna. The group velocity of light becomes slow underneath the antenna due to the Plasmon effect. It is possible that this affects the velocity of the parallel electric component, thereby resulting in slow velocity and excitation of the SPHP modes.

The results shown in Fig. (2b) are evident: the electric field intensity which a natural SiO_2 layer felt was weak with an increase in the thickness of Al_2O_3. Reflectivity in the high wave number range dropped as the Al_2O_3 layer was thick, but it did not vary in a striking manner below ~1050 cm^{-1}. This was because this range corresponded to the stop band of Al_2O_3 [23]. The field intensity in parallel planes below and at the air/substrate interface was calculated using the FDTD method. When the Al_2O_3 layer thickness becomes 10 nm, it drops off to about 10% of the intensity at the surface, which was in reasonable agreement with the experimental results.

4. Conclusions

The vertical distribution of the electric field enhancement produced by optical antennas could be experimentally confirmed. The combination of the antenna and a quantum cascade laser would yield attractive mid-infrared microscopic analysis to detect a solid state surface. In this work, slot antenna arrays were formed on a thin Al_2O_3 layer grown by atomic layer deposition on a silicon substrate. Reflectivity spectra measured in the mid-infrared range showed characteristic aspects, presumably caused by the surface phonon polariton of a SiO_2 layer naturally formed on the Si substrate. When the Al_2O_3 layer thickness was 6 nm, such spectral features disappeared. In this way, we could estimate experimentally the electric field distribution normal to the surface of the substrate.

References

[1] K. L. Wong, *Compact and Broadband Microstrip Antennas*. New York: Wiley, 2002.

[2] M. Kahrizi, T. K. Sarkar, and Z. A. Maricevic, "Analysis of a wide radiating slot in the ground plane of a microstrip line," *IEEE Trans. Antennas Propag.*, vol. 41, no. 1, pp. 29–37, Jan. 1993.

[3] S.-W. Qu, J.-L Li, J.-X. Chen, and Q. Xue, "Ultra wideband strip-loaded circular slot antenna with improved radiation patterns," *IEEE Trans. Antennas Propag.*, vol. 55, no. 11, pp. 3348–3353, Nov. 2007.

[4] P. Li, J. Liang, and X. Chen, "Study of printed elliptical/circular slot antennas for ultra wideband applications," *IEEE Trans. Antennas Propag.*, vol. 54, no. 6, pp. 1670–1675, Jun. 2006.

[5] W.-S. Chen and F.-M. Hsieh, "A broadband design for a printed isosceles triangular slot

antenna for wireless communications," *Microw. J.*, vol. 48, no. 7, pp. 98–112, Jul. 2007.
[6] J. Y. Sze and K. L. Wong, "Bandwidth enhancement of a microstrip line-fed printed wide-slot antenna," *IEEE Trans. Antennas Propag.*, vol. 49, no. 7, pp. 1020–1024, Jul. 2001.
[7] T. Dissanayake and K. P. Esselle, "UWB performance of compact L-shaped wide slot antennas," *IEEE Trans. Antennas Propag.*, vol. 56, no. 4, pp. 1183–1187, Apr. 2008.
[8] S. Chen, P. Hallbjorner, and A. Rydberg, "Printed slot planar inverted cone antenna for ultra wideband applications," *IEEE Antennas Wireless Propag. Lett,* vol. 7, pp. 18–21, 2008.
[9] S.-W. Qu, C. Ruan, and B.-Z. Wang, "Bandwidth enhancement of wide-slot antenna fed by CPW and microstrip line," *IEEE Antennas Wireless Propag. Lett.*, vol. 5, pp. 15–17, 2006.
[10] W.-L. Chen,G.-M. Wang, and C. X. Zhang, "Bandwidth enhancement of a microstrip-line-fed printed wide-slot antenna with a fractal-shaped slot," *IEEE Trans. Antennas Propag.*, vol. 57, no. 7, pp. 2176–2179, Jul. 2009.
[11] D. D. Krishna, M. Gopikrishna, C. K. Aanandan, P. Mohanan, and K. Vasudevan, "Compact wideband Koch fractal printed slot antenna," *Microw. Antennas Propag.*, vol. 3, no. 5, pp. 782–789, Aug. 2009.
[12] J.-Y. Jan and J.-W. Su, "Bandwidth enhancement of a printed wide-slot antenna with a rotated slot," *IEEE Trans. Antennas Propag.*, vol. 53, no. 6, pp. 2111–2114, Jun. 2005.
[13] C. T. P. Song, P. S. Hall, H. Ghafouri-Shiraz, and D. Wake, "Fractal stacked monopole with very wide bandwidth," *Electron. Let*, vol. 35, no. 12, pp. 945–946, 1999.
[14] J. Anguera, E. Martínez, C. Puente, and E. Rozan, "The fractal Hilbert monopole: A two-dimensional wire," *Microw. Opt. Technol. Lett.*, vol. 36, no. 2, pp. 102–104, Jan. 2003.
[15] J. P. Gianvittorio and Y. Rahmat-Samii, "Fractal antennas: A novel antenna miniaturization technique, and applications," *IEEE Antennas Propag. Mag.*, vol. 44, no. 1, pp. 20–36, Feb. 2002.
[16] C. Puente, J. Anguera, C. Borja, and J. Soler, "Fractal-shaped antennas and their application to GSM 900/1800," *J. Inst. British Telecommun. Eng.*, vol. 2, pt. 3, Jul. 2001.
[17] K.B. Crozier, A. Sundaramurthy, G.S. Kino, and C.F. Quate, *J. Appl. Phys.*, 2003, 94, 4632.
[18] M. Brehm, T. Taubner, R. Hillenbrand, and F. Keilmann, *Nano Lett.,* 2006, 6, 1307.
[19] V.D. Kumar and K. Asakawa,, *Photon. Nanostruct.,* 2009, 7, 161.
[20] K. Ishikawa, H. Ogawa, and S. Fujimura, *J. Appl. Phys*., 1999, 85, 4076.
[21] F. Neubrech, D. Weber, D. Enders, T. Nagao, and A. Pucci, *J. Phys. Chem.C*, 2011, 7299.
[22] M.G. Cottam and D.R. Tilley, *Introduction to surface and supperlattice excitations* 2nd ed., Bristol and Philadelphia: Institute of Physics Publishing, 2005.
[23] D. Palik, *Handbook of optical constants of solids* Ⅲ, San Diego: Academic Press, 1998.